nature biotechnology

Supplementary information

https://doi.org/10.1038/s41587-026-03197-y

Optimized R2 retroelement complexes for DNA insertion into plant genomes

In the format provided by the authors and unedited

SUPPLEMENTARY INFORMATION

Table of Contents

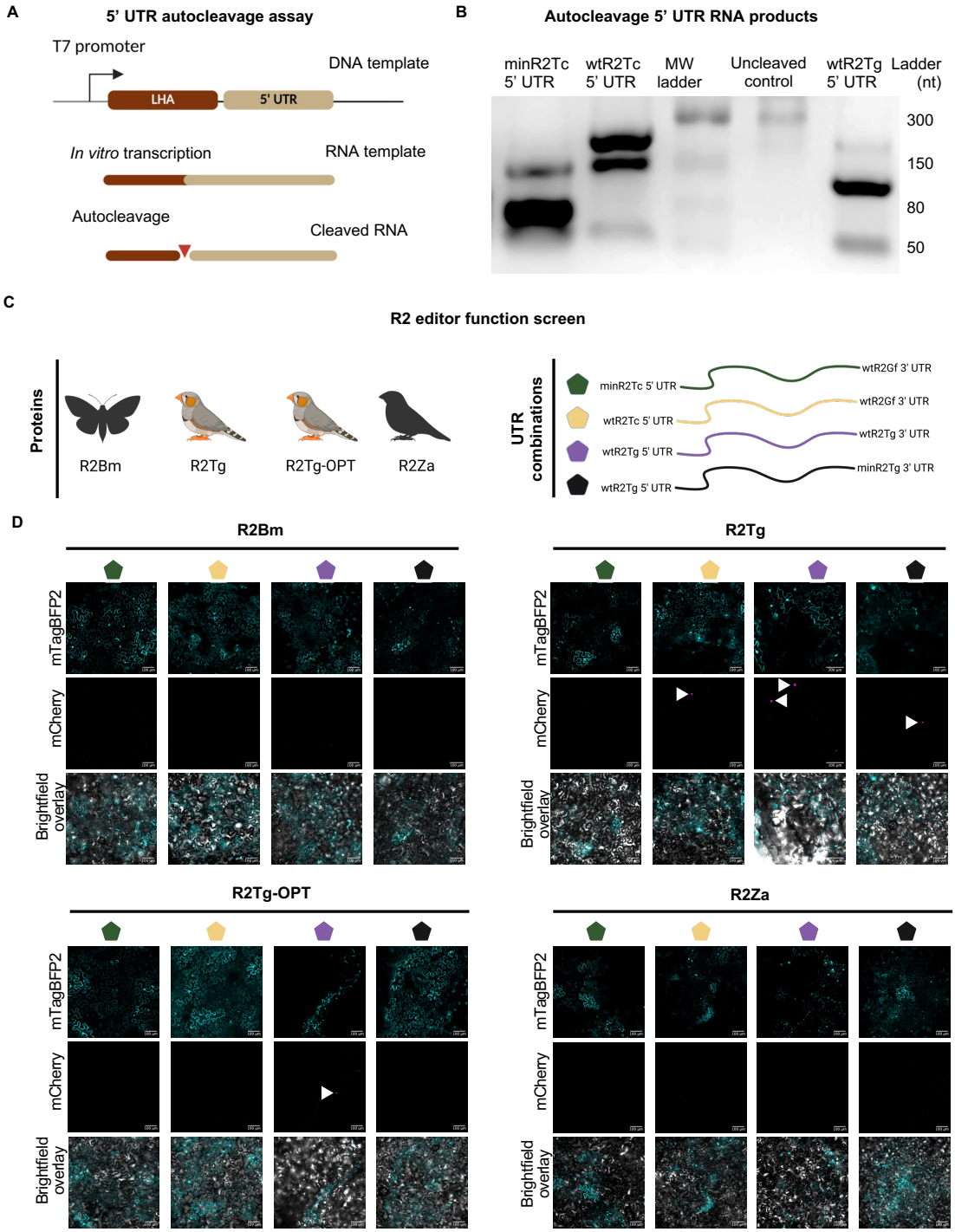

Supplementary Figure 1. Validation of 5′ UTR autocleavage activity and functional screening of R2 editors. (A) Schematic of the *in vitro* 5′ UTR autocleavage assay. 25s rDNA 100 bp homology sequence was fused to R2 5′ UTRs downstream of a T7 promoter, which was transcribed *in vitro* and assayed for autocleavage activity based on fragment sizes. **(B)** 2% TAE agarose gel showing cleavage products of three 5′ UTR variants: minimal *Tribolium castaneum* (minR2Tc), wild-type *T. castaneum* (wtR2Tc), and wild-type *Taeniopygia guttata* (wtR2Tg). Arrowheads indicate expected fragments. Band sizes match predicted cleavage outcomes: minR2Tc (uncleaved 177 nt, 105 nt, 72 nt), wtR2Tc (uncleaved 265 nt, 193 nt, 72 nt), and wtR2Tg (uncleaved 275 nt, 203 nt, 72 nt). A 300 nt synthetic RNA template was used to denote uncleaved template sizes. Representative of 3 independent experiments with similar results. **(C)** Representative confocal microscopy images from the R2 editor function screen in *N. benthamiana* leaves, displaying mTagBFP2 (cyan, delivery marker) and mCherry (magenta, reporter of successful integration) fluorescence for four R2 protein variants: R2Bm (*Bombyx mori*), R2Tg (*T. guttata*), codon-optimized R2Tg-OPT, and R2Za (*Zonotrichia albicollis*) combined with four donor RNA architectures that pair distinct 5′/3′-UTR sets: Green: minR2Tc 5′ UTR + wtR2Gf 3′ UTR (minimal *Tribolium castaneum* 5′ UTR with wild-type *Geospiza fortis* 3′ UTR); Yellow: wtR2Tc 5′ UTR + wtR2Gf 3′ UTR (wild-type *T. castaneum* 5′ UTR with wild-type *G. fortis* 3′ UTR); Purple: wtR2Tg 5′ UTR + wtR2Tg 3′ UTR (wild-type *T. guttata* UTRs); and Black: minR2Tg 5′ UTR + minR2Tg 3′ UTR (wild-type *T. guttata* 5’ UTR and minimal *T. guttata* 3’ UTR). Scale bars, 100 µm. Arrowheads indicate a nuclear mCherry signal from the R2-mediated targeted integration. Representative of 3 independent experiments with similar results. LHA: left homology arm, UTR: untranslated region. Partially created in BioRender. Demirer, G. (2026) https://BioRender.com/2c5a2fi.

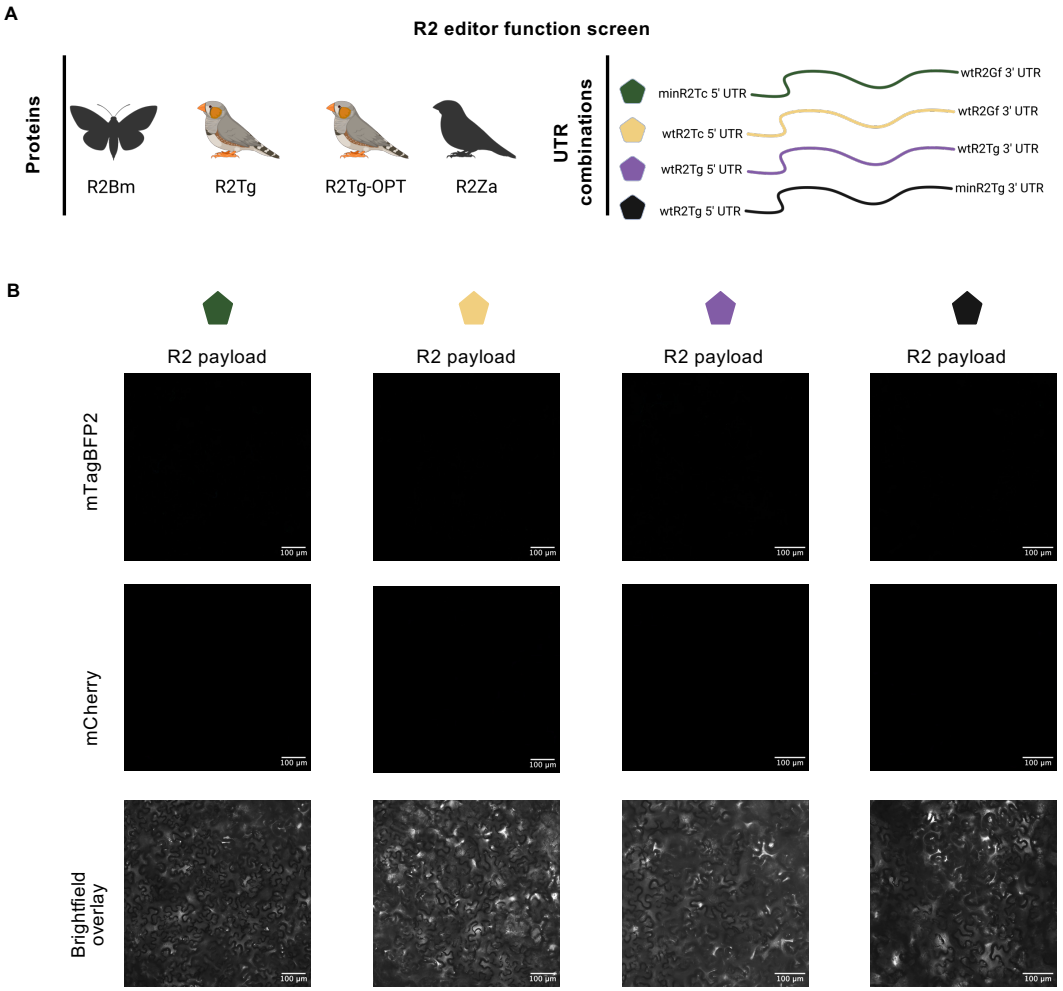

Supplementary Figure 2. Negative control samples from the functional screening of R2 editors. (A) Schematic of the R2 editor function screen showing four R2 protein variants, R2Bm (*Bombyx mori*), R2Tg (*Taeniopygia guttata*), R2Tg-OPT (a rationally improved variant of R2Tg), and R2Za (*Zonotrichia albicollis*). R2 variants are paired with different 5′ and 3′ UTR combinations with distinct 5′/3′-UTR sets: Green: minR2Tc 5′ UTR + wtR2Gf 3′ UTR (minimal *Tribolium castaneum* 5′ UTR with wild-type *Geospiza fortis* 3′ UTR); Yellow: wtR2Tc 5′ UTR + wtR2Gf 3′ UTR (wild-type *T. castaneum* 5′ UTR with wild-type *G. fortis* 3′ UTR); Purple: wtR2Tg 5′ UTR + wtR2Tg 3′ UTR (wild-type *T. guttata* UTRs); and Black: minR2Tg 5′ UTR + minR2Tg 3′ UTR (wild-type *T. guttata* 5’ UTR and minimal *T. guttata* 3’ UTR). All R2 payload cassettes used in the R2 editor function screen carry 100-bp left and right homology arms. **(B)** Representative confocal fluorescence microscopy images of *N. benthamiana* leaves infiltrated with constructs encoding only the payload cassettes and lacking the R2 protein effector. mTagBFP2 (cyan) reports transformation, and mCherry (magenta) reports R2-mediated integration in the presence of an R2 protein effector. Scale bars, 100 µm. Representative of 3 independent experiments with similar results. Partially created in BioRender. Demirer, G. (2026) https://BioRender.com/axy32jo.

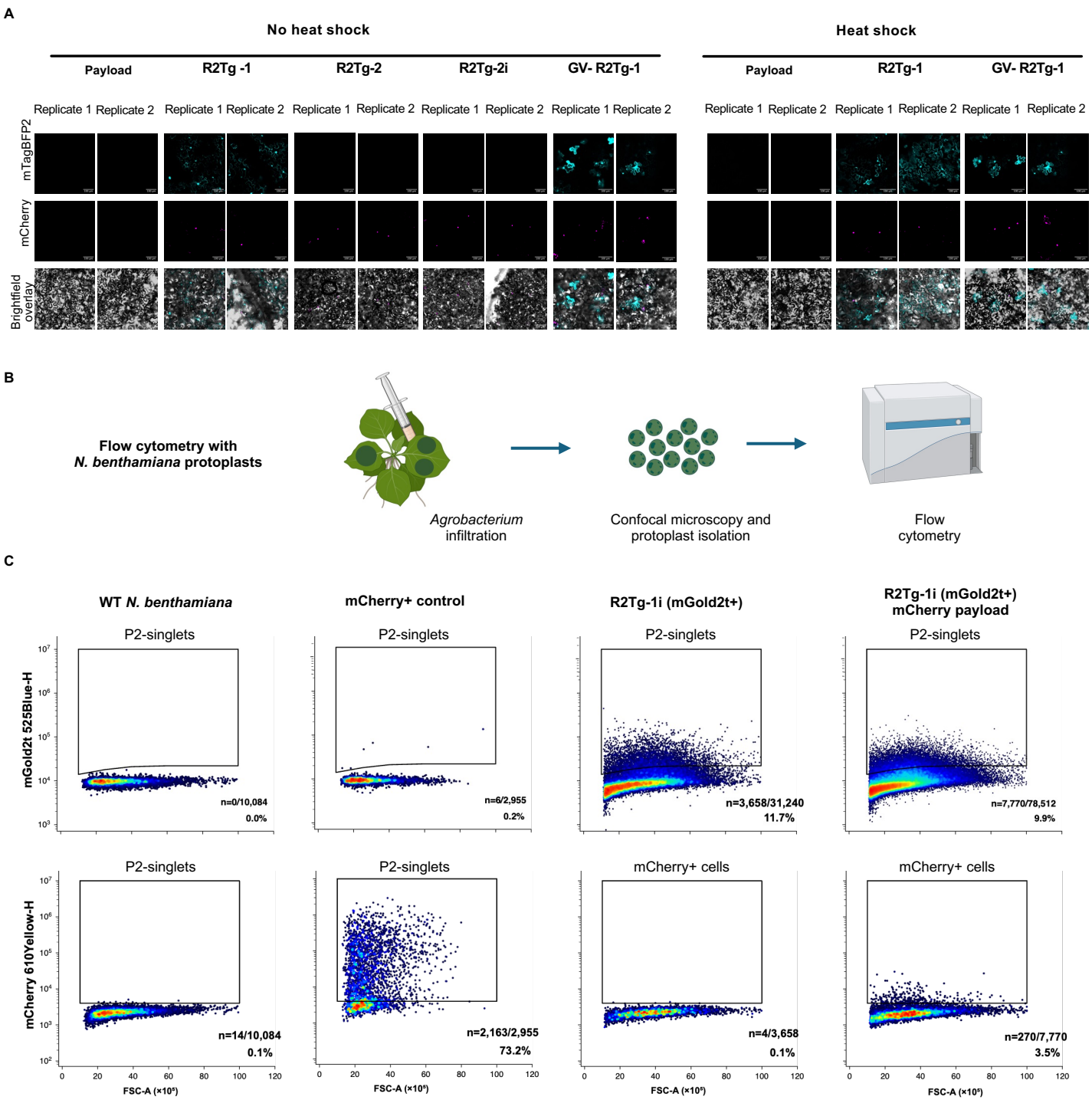

Supplementary Figure 3. Confocal imaging and flow cytometry analysis of R2Tg editor systems in infiltrated leaves and plant protoplasts. (A) Representative confocal fluorescence images of *Nicotiana benthamiana* leaves infiltrated with R2Tg constructs expressing the R2Tg protein and donor template from a single plasmid, from separate plasmids, or an intronized R2Tg expression cassette, together with GV-R2Tg constructs. Leaves were imaged either without heat shock or after a 3-day heat shock that began 2 days after infiltration. mTagBFP2 (cyan) marks construct delivery, mCherry (magenta) reports payload integration and expression, and brightfield overlay is shown in the bottom row. Two biological replicates are shown for each condition. Scale bars, 100 µm. **(B)** Schematic of *N. benthamiana* leaf infiltration and protoplast isolation workflow. **(C)** Flow cytometry plots of *N. benthamiana* protoplasts showing mGold2t and mCherry fluorescence following infiltration with WT Nb, mCherry positive control, R2Tg intronized (mGold2t reporter), and R2Tg intronized (mGold2t) with mCherry payload constructs. For WT Nb and mCherry positive control samples, plots are gated on P2 singlets. For R2Tg constructs, mCherry plots are gated on mGold2t$^+$ cells. Gating strategy is described in Supplementary Figure 14. Event counts and gate percentages are shown in the lower right corner of each panel. Representative of 3 independent experiments with similar results. mGold2t$^+$: mGold2t-positive population; mCherry$^+$: mCherry-positive population; GV: geminiviral replicon; R2Tg: *Taeniopygia guttata* R2 element; R2Tg-1: single-plasmid R2Tg system; R2Tg-2: dual-plasmid R2Tg system; R2Tg-2i: dual-plasmid intronized R2Tg system; GV-R2Tg-1: geminiviral single-plasmid R2Tg system; 525Blue-H: channel detecting mGold2t fluorescence (excitation 488 nm, emission ~530 nm); 610Yellow-H: channel detecting mCherry fluorescence (excitation 561 nm, emission ~610 nm). Partially created in BioRender. Demirer, G. (2026) https://BioRender.com/uazuy49.

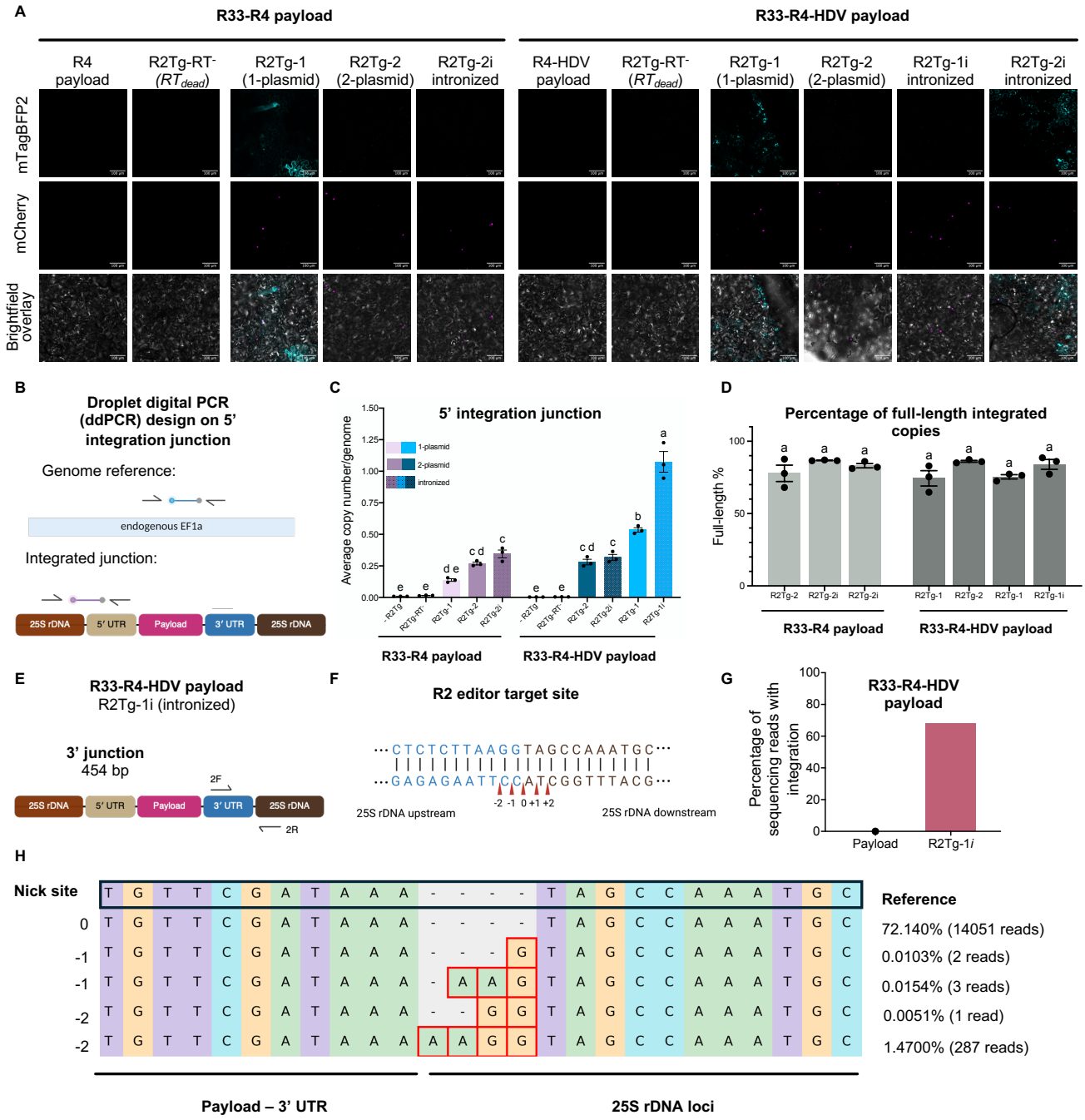

Supplementary Figure 4. Characterization of R4 and R4-HDV payloads in *N. benthamiana* by ddPCR and NGS. (A) Confocal fluorescence microscopy of *N. benthamiana* leaves co-infiltrated with R2Tg and either R4 or R4-HDV payloads. mTagBFP2 (cyan) marks delivery; mCherry (magenta) indicates reporter activation. Scale bars, 100 µm. Representative of 3 independent experiments with similar results. **(B)** Schematic of droplet digital PCR (ddPCR) assay for quantification of average insertion copy number per genome using primers and a probe specific to the integrated 5′ junction, normalized against an endogenous *NbEF1α* control locus. **(C)** Quantification of average insertion copy number per genome by ddPCR. Bars represent mean ± S.E.M. from 3 independent biological replicates. Statistical analysis is performed using ordinary one-way ANOVA with Tukey's HSD multiple-comparison test. Different letters denote statistically significant differences; exact p-values for all pairwise comparisons are provided in the Source Data file. **(D)** Quantification of full-length integrated products with intact 3' and 5' junctions detected by ddPCR. Bars represent mean ± S.E.M. from 3 independent biological replicates. Statistical analysis is performed using ordinary one-way ANOVA with Tukey's HSD multiple-comparison test. Different letters denote statistically significant differences; exact p-values for all pairwise comparisons are provided in the Source Data file. **(E)** Schematic of the 3′ junction showing the R2 payload flanked by 5′ and 3′ UTRs inserted into the 25S rDNA locus. Primer 2F anneals within the 3′ UTR, and primer 2R anneals downstream in native 25S rDNA. **(F)** Schematic of R2 target site in the 25s rDNA locus showing nucleotides derived from upstream (blue) and downstream (brown) of the 25S rDNA target, arrowheads mark the inferred bottom strand nick positions for the R2 protein. **(G)** Percentage of sequencing reads containing integrated junctions in R4-HDV payload paired with R2Tg-1i. **(H)** Representative amplicon sequencing reads aligned to the reference 3′ junction show the indel profile. Each row corresponds to a unique read, with nucleotide identity indicated by color (A: green, T: purple, C: blue, G: orange). Red boxes mark extra bases at the 3′ junction, which arise from R2 endonuclease nicking 1-2 bases upstream of the canonical integration site and/or non-templated addition of A nucleotides prior to the start of the 3′ UTR. Results are representative of 3 independent experiments with similar results. R2Tg: *Taeniopygia guttata* R2 element, rDNA: Ribosomal DNA, UTR: Untranslated region, HDV: Hepatitis Delta Virus ribozyme, R4: 4-nucleotide sequence derived from the 25S rDNA region immediately downstream of the target site, RT: Reverse transcriptase. Partially created in BioRender. Demirer, G. (2026) https://BioRender.com/80p5q73.

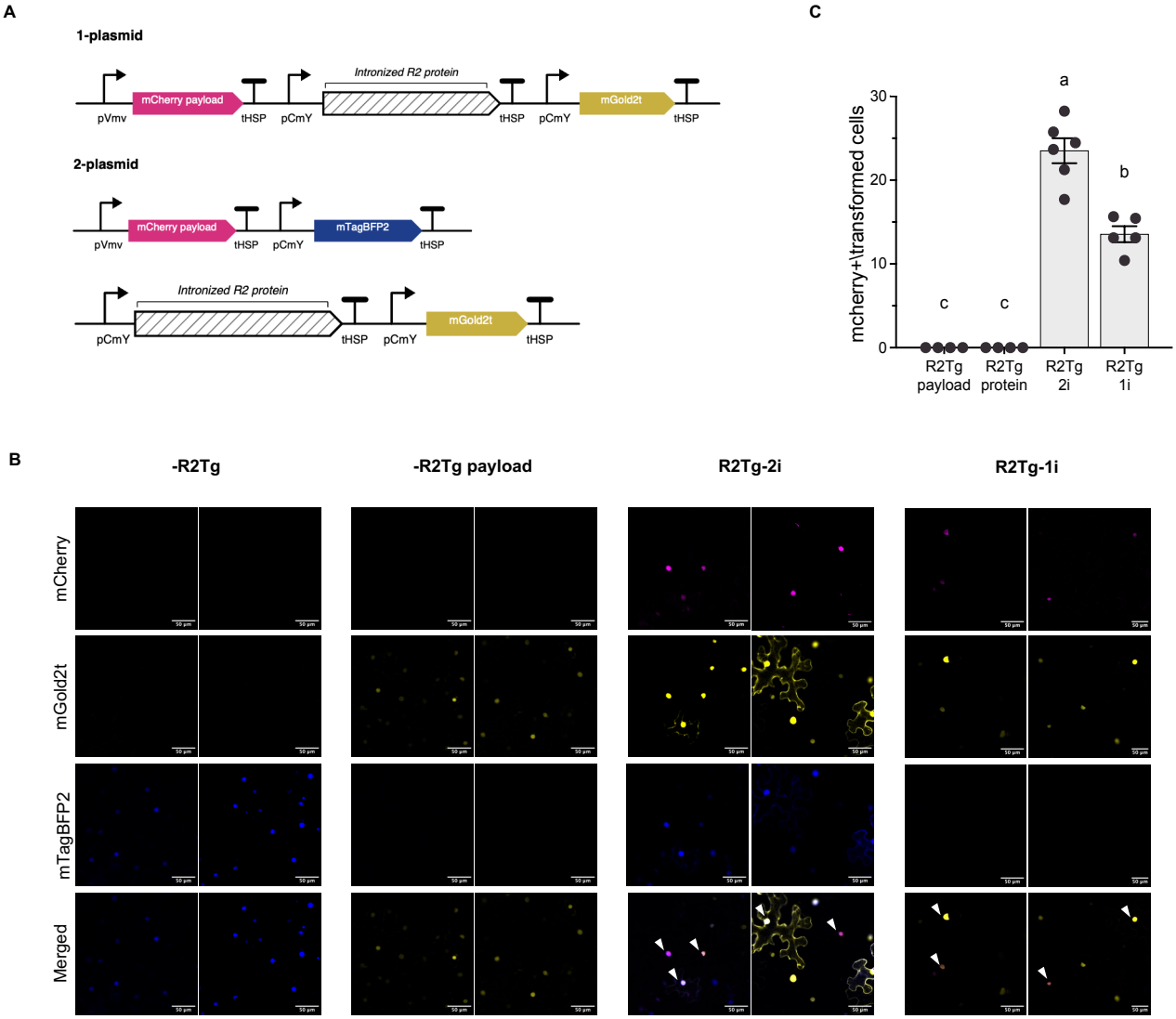

Supplementary Figure 5. Confocal microscopy quantification of mCherry integration. (A) Two delivery formats were tested: 1-plasmid system encoding both the R2Tg intronized protein and the payload cassette with the mGold2t transformation reporter, and 2-plasmid system with the R2Tg intronized protein and the payload cassette delivered on separate *Agrobacterium* T-DNAs carrying mGold2t and mTagBFP2 transformation reporters, respectively. All markers are localized to the nuclei. **(B)** Representative confocal fluorescence microscopy images of *Nicotiana benthamiana* leaves transformed with constructs from panel A, imaged 3 days post-transformation. Scale bars, 50 µm. Arrows indicate nuclear-localized mCherry signal colocalized with transformation marker(s). Representative of 3 independent experiments with similar results. **(C)** Quantification of mCherry+ nuclei normalized by transformation marker(s). Bars represent mean ± S.E.M. n=4 independent biological replicates for R2Tg payload and protein, n=6 independent biological replicates for R2Tg-2i, and n=5 independent biological replicates for R2Tg-1i. P values were obtained using ordinary one-way ANOVA with Tukey HSD multiple comparison test. Different letters denote statistically significant differences; exact p-values for all pairwise comparisons are provided in the Source Data file.

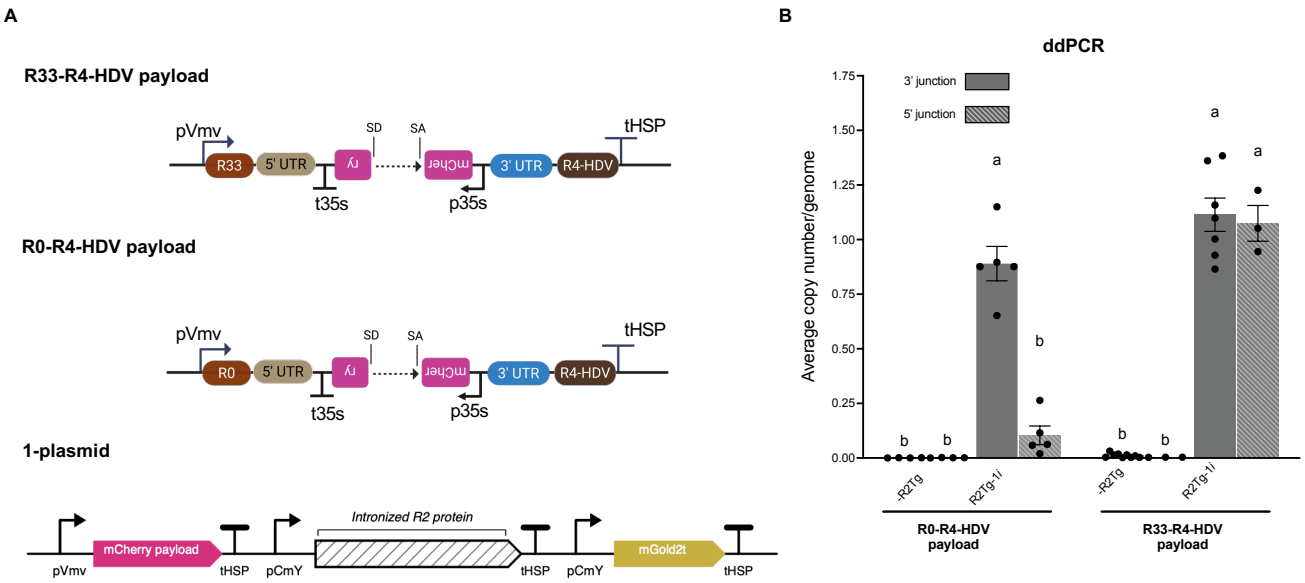

Supplementary Figure 6. Addition of rDNA sequence homology to the upstream of the 5' UTR enables precise full-length 5' junction formation. (A) Schematic of the R0-R4-HDV and R33-R4-HDV payload variants. Both payloads were delivered with the 1-plasmid system encoding the intronized R2Tg protein and mGold2t reporter for transformation. All fluorescent proteins are nucleus-localized. **(B)** ddPCR quantification of targeted insertion copy frequency at the 3' junction (solid bars) and 5' junction (hatched bars), normalized to the endogenous *RDR1* reference locus in *Nicotiana benthamiana* leaves. Bars represent mean ± S.E.M. from at least 3 independent biological replicates. Precise n numbers for each condition are provided in the Source Data file. Statistical analysis was performed using ordinary one-way ANOVA with Tukey's HSD multiple-comparison test. Different letters denote statistically significant differences; exact p-values for all pairwise comparisons are provided in the Source Data file. R2Tg: *Taeniopygia guttata* R2 element, rDNA: ribosomal DNA, UTR: untranslated region, HDV: hepatitis delta virus ribozyme, R0: no upstream rDNA homology arm, R4: 4-nt downstream 25S rDNA homology, R33: 33-nt upstream 25S rDNA homology, wt: wild type, pVmv: Cassava vein mosaic virus promoter, tHSP: *A. thaliana* HSP18.2 terminator, pCmY: CmYLCV6 promoter, p35s: CaMV 35S promoter, t35s: CaMV 35S terminator, SD: splice donor, SA: splice acceptor. Partially created in BioRender. Demirer, G. (2026) https://BioRender.com/8zcnvjf .

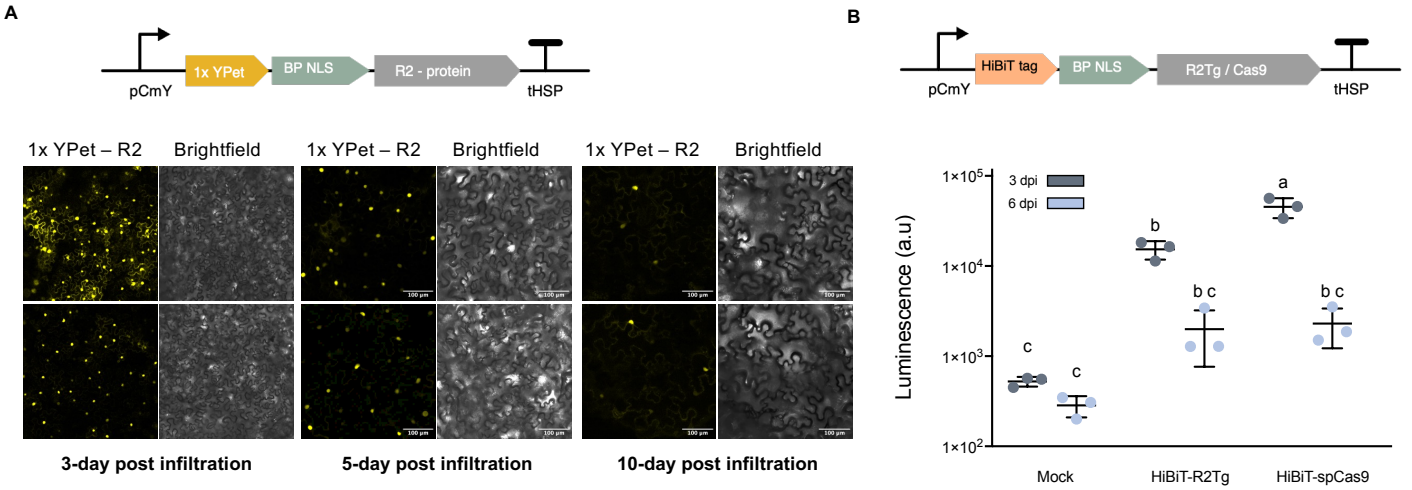

Supplementary Figure 7. Time-course characterization of R2Tg protein expression in leaves. (A) Top: construct used for fluorescence-based detection of R2 protein expression. The R2 coding sequence was expressed under the pCmY promoter and tagged at the N-terminus with a 1×YPet fluorescent protein and BP NLS, followed by the tHSP terminator. Bottom: representative confocal microscopy images of *N. benthamiana* leaves following transient *A. tumefaciens* infiltration at 3-, 5-, and 10-days post infiltration (dpi) from 3 independent experiments with similar results. Scale bars, 100 µm. **(B)** Top: construct used for luminescence-based detection of R2 protein expression. The R2 coding sequence or Cas9 control was expressed under the pCmY promoter and tagged at the N-terminus with a HiBiT peptide for luminescence detection and a bipartite (BP) nuclear localization signal (NLS) for nuclear targeting, followed by the tHSP terminator. Bottom: quantification of R2 protein abundance using the HiBiT-tag constructs. Individual plant biological replicates were sampled at 3- and 6-days post-infiltration (dpi). Luminescence values (RLU) from biological replicates are presented as a scatter plot, with mean ± SD shown, n=3. Statistical analysis was performed using ordinary one-way ANOVA with Tukey's HSD multiple-comparison test. Different letters denote statistically significant differences; exact p-values for all pairwise comparisons are provided in the Source Data file.

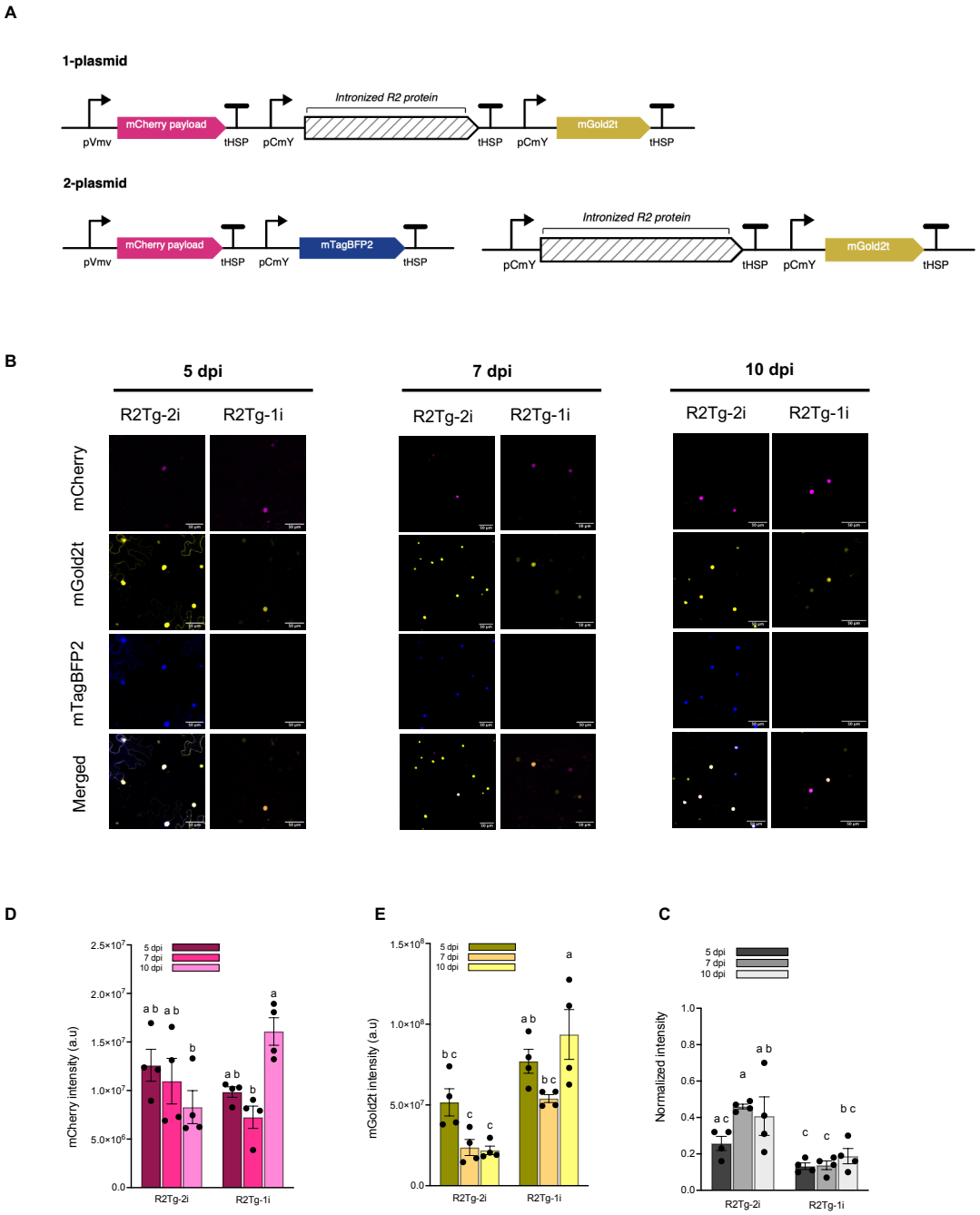

Supplementary Figure 8. Time-course characterization of inserted mCherry expression from rDNA. **(A)** Two delivery formats were tested: a 1-plasmid system encoding both the R2Tg intronized protein and the payload cassette with the mGold2t transformation marker, and a 2-plasmid system with the R2Tg intronized protein and the payload cassette delivered on separate *Agrobacterium* T-DNAs carrying mGold2t and mTagBFP2 markers, respectively. All fluorescent proteins are nuclear-localized. **(B)** Representative confocal fluorescence microscopy images of *N. benthamiana* leaves transformed with constructs from panel A at 5-, 7-, and 10-days post-infiltration. mTagBFP2 (blue, transformation marker), (mGold2t, transformation marker), mCherry (magenta, R2-mediated integration reporter), and all channels merged from 4 independent biological replicates with similar results. Scale bars, 50 µm. Quantification of **(C)** integrated mCherry fluorescence intensity, **(D)** mGold2t transformation marker fluorescence intensity, and **(E)** mCherry normalized by mGold2t transformation marker fluorescence intensity at 5-, 7-, and 10-days post infiltration. Bars represent mean ± S.E.M. n=4 independent biological replicates. P values were obtained using ordinary one-way ANOVA with Tukey HSD multiple comparison test. Different letters denote statistically significant differences; exact p-values for all pairwise comparisons are provided in the Source Data file.

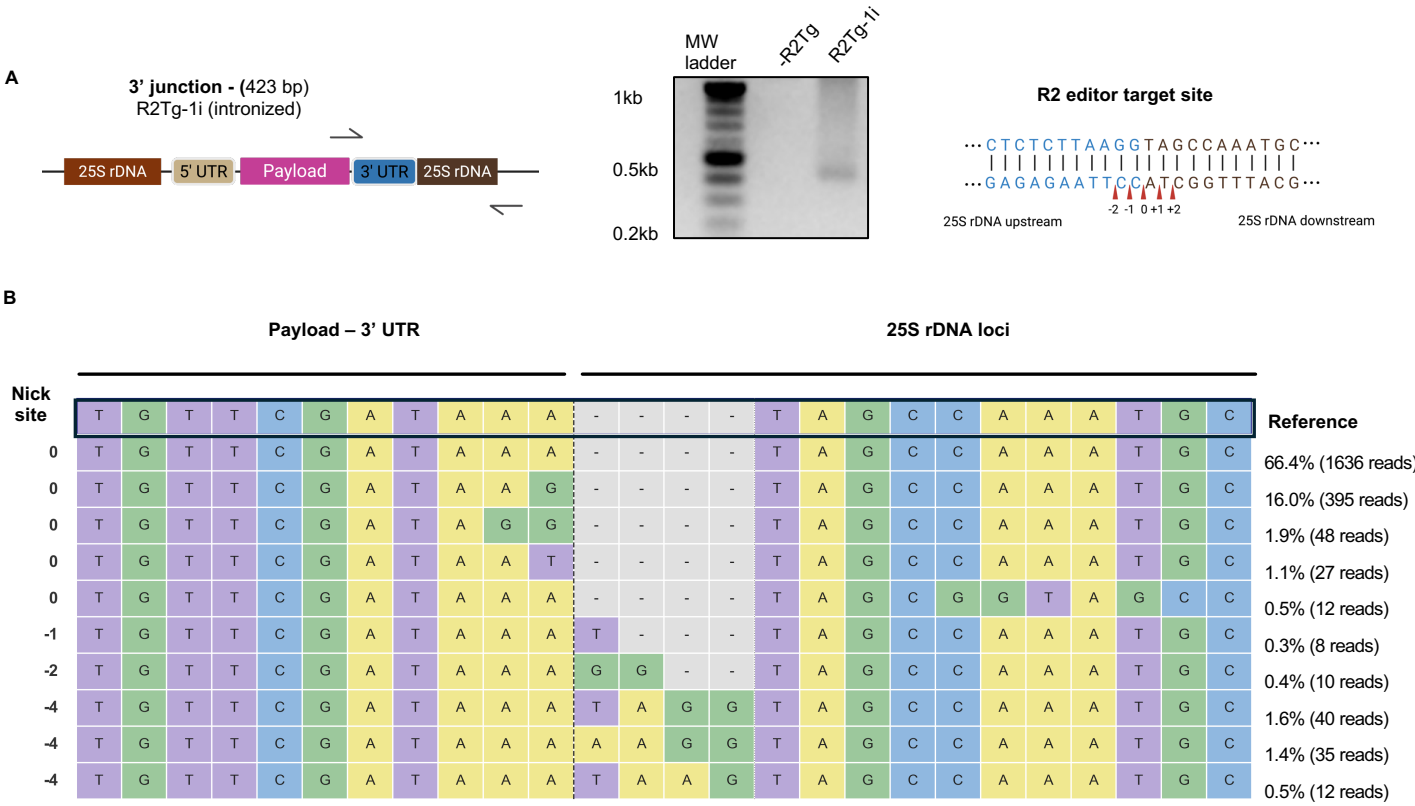

Supplementary Figure 9. Characterization of R2-mediated payload insertion at the 25S rDNA locus in *Arabidopsis thaliana*. (A) Schematic of the 3' junction PCR amplicon (423 bp) used to detect R2Tg-1i-mediated targeted insertion, alongside a representative gel image showing amplification in R2Tg-1i-transformed plants but not the R2Tg negative control from 3 independent biological replicates with similar results. The 3' integration junction site sequence is shown, with arrows indicating the range of observed nick sites relative to the canonical cleavage site. **(B)** Nanopore amplicon sequencing of the 3' integration junction from a representative biological replicate (n=2 total). Each row displays a unique read alignment spanning the payload 3' UTR-25S rDNA junction, with the nick site position indicated on the left and read frequency on the right. Dashes indicate deletions; colored nucleotides reflect base identity at each position. Representative of 3 independent experiments with similar results. R2Tg: *Taeniopygia guttata* R2 element, rDNA: ribosomal DNA, UTR: untranslated region, MW: molecular weight, bp: base pairs. Partially created in BioRender. Demirer, G. (2026) https://BioRender.com/puu01kf.

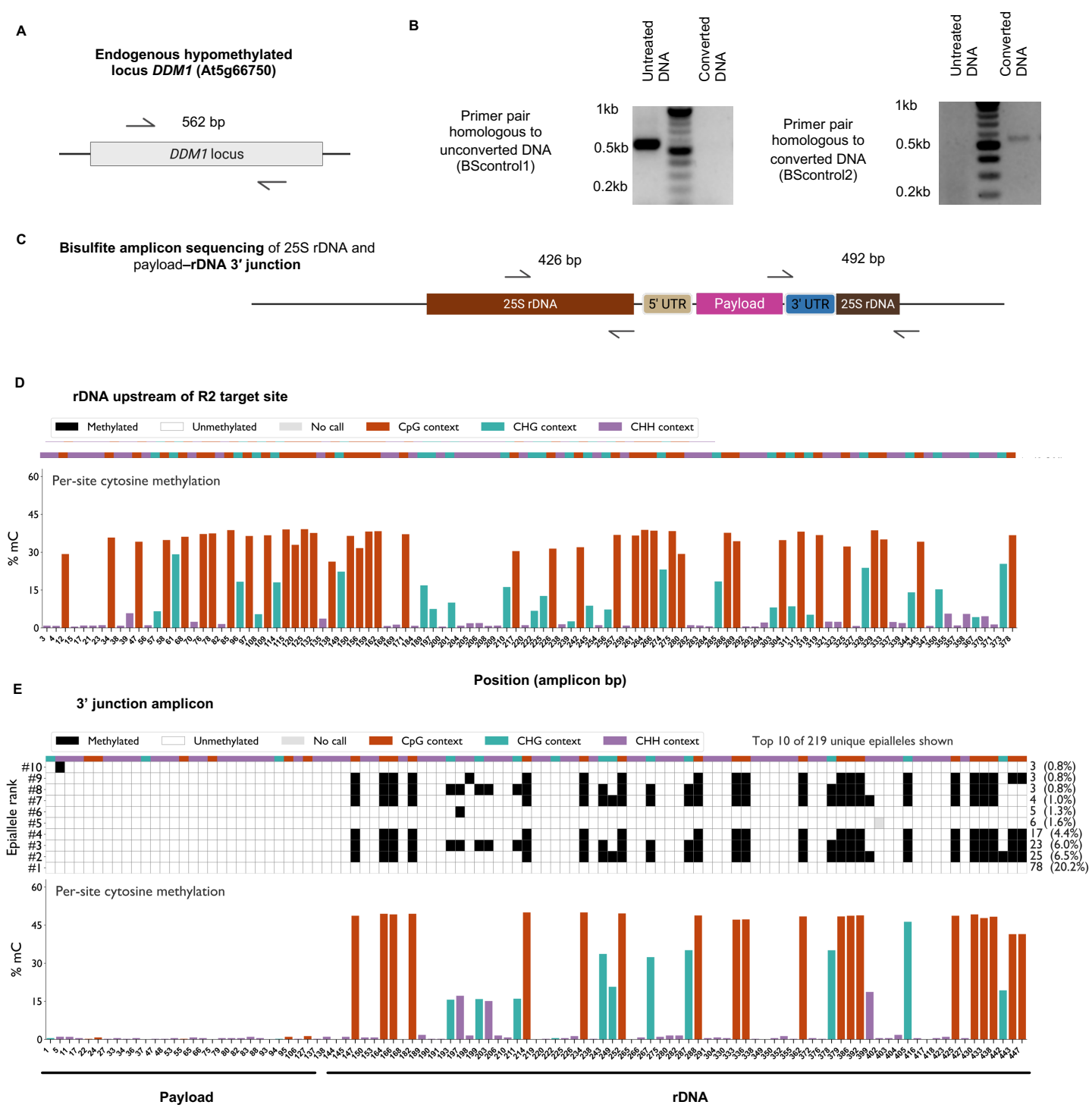

Supplementary Figure 10. Cytosine methylation profile of the integrated payload at the 25S rDNA target site in *Arabidopsis thaliana*. **(A)** Schematic of the endogenous hypomethylated *DDM1* locus, amplified as a bisulfite conversion control (562 bp). **(B)** Gel images confirming bisulfite conversion efficiency using primer pairs homologous to unconverted (BScontrol1) and bisulfite-converted (BScontrol2) DNA. Representative of 3 independent experiments with similar results. **(C)** Schematic of bisulfite amplicon targets: the 25S rDNA upstream region (426 bp) and the payload-rDNA 3' junction (492 bp), used to profile cytosine methylation at and flanking the integration site from bisulfite conversion of DNA, followed by targeted PCR amplification with degenerate primers and Nanopore sequencing. **(D)** Per-site cytosine methylation (% mC) across the rDNA upstream of the R2 target site, shown by sequence context (CpG, CHG, CHH). Representative of 3 independent experiments with similar results. **(E)** Methylation profile of the 3' junction amplicon. The upper panel displays the top 10 of 219 unique epialleles ranked by frequency, with read counts and percentages indicated on the right. The lower panel shows per-site % mC across the payload and rDNA regions by sequence context. Representative of 3 independent experiments with similar results. DDM1: Decrease in DNA Methylation 1, rDNA: ribosomal DNA, UTR: untranslated region, mC: methylated cytosine, CpG/CHG/CHH: cytosine methylation sequence contexts, BS: bisulfite, bp: base pairs. Partially created in BioRender. Demirer, G. (2026) https://BioRender.com/gnmsh3l.

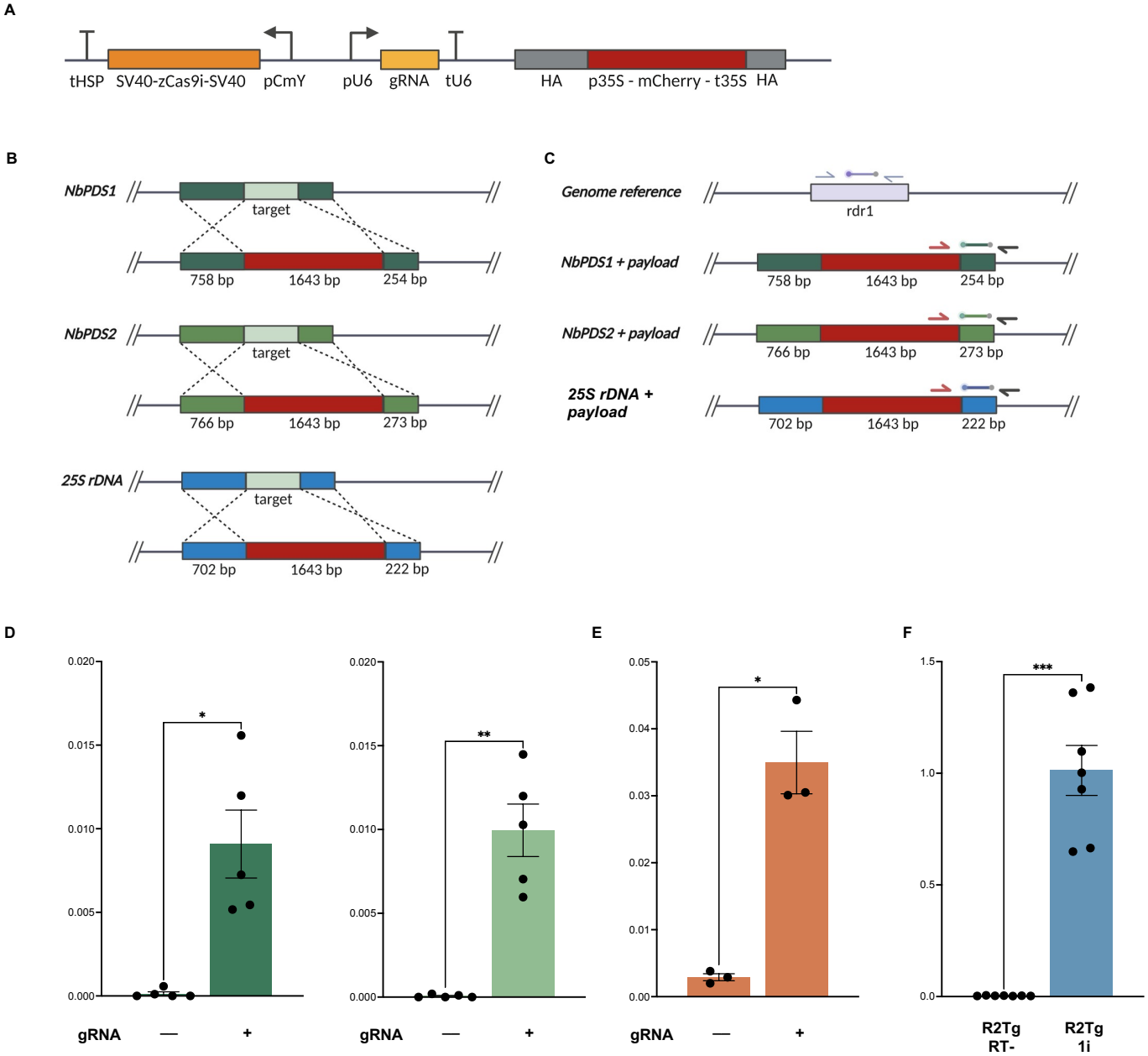

Supplementary Figure 11. R2 integration efficiency comparison with Cas9 HDR. (A) Schematic of the Cas9-gRNA-payload construct. **(B)** HDR strategy for targeted integration of the payload at the *NbPDS1, NbPDS2,* and *Nb 25S rDNA* loci. Dashed lines indicate homology-directed repair between genomic target sites and homology arms. **(C)** ddPCR assay design for quantifying genome reference alleles and correctly integrated alleles. **(D)** Quantification of Cas9-HDR mediated payload integration efficiency at *NbPDS1* and *NbPDS2*. Bars represent mean ± S.E.M. from 6 independent biological replicates. **(E)** Quantification of Cas9-HDR mediated payload integration efficiency at *Nb 25S rDNA*. Bars represent mean ± S.E.M. from 3 independent biological replicates. **(F)** Quantification of R2Tg-mediated integration efficiency. Bars represent mean ± S.E.M. from 7 independent biological replicates. Statistical significance was analyzed using Unpaired two-tailed t-test with Welch's correction(***$p < 0.001$, **$p < 0.01$, *$p < 0.05$), exact p-values for pairwise comparison are provided in the Source Data file. pCmY: CmYLCV6 promoter derived from Cestrum yellow leaf-curling virus, tHSP: *Arabidopsis thaliana* heat shock protein 18.2 terminator, p35s: Cauliflower mosaic virus 35S promoter, t35s: Cauliflower mosaic virus 35S terminator, HA: homology arm, R2Tg: *Taeniopygia guttata* R2 element, R2Tg-1i: intronized R2Tg, RT: reverse transcriptase.

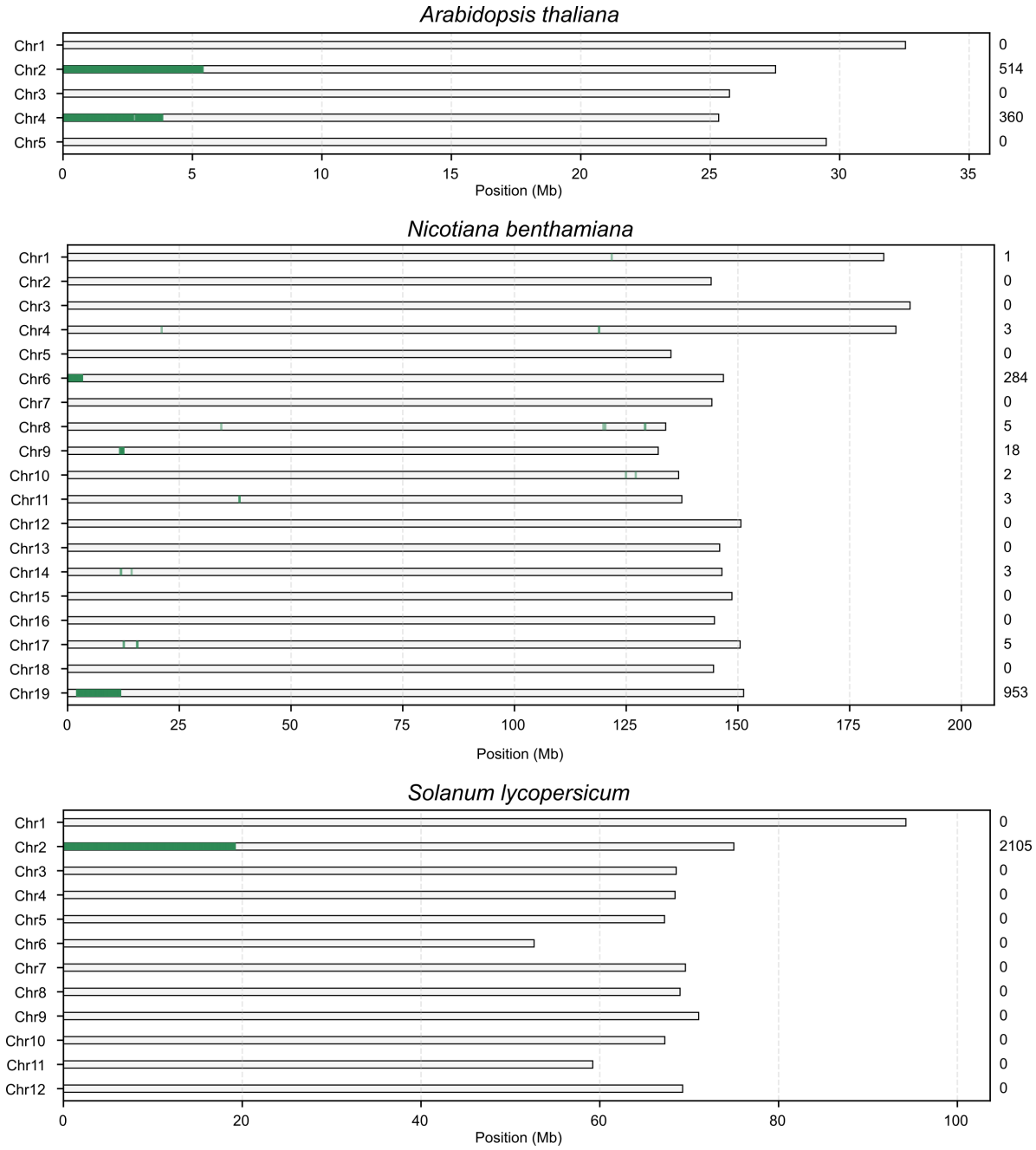

Supplementary Fig 12: Chromosomal distribution of all predicted R2-compatible 25S rDNA sequences in *Arabidopsis thaliana*, *Nicotiana benthamiana*, and *Solanum lycopersicum* genomes. 25S rDNA loci were identified and filtered to retain only sequences containing the conserved R2 recognition/cleavage motif. For each species, chromosomes are shown as horizontal bars (x-axis in Mb), with green marks indicating the genomic positions of R2-compatible 25S sites; numbers at right indicate the total number of sites per chromosome.

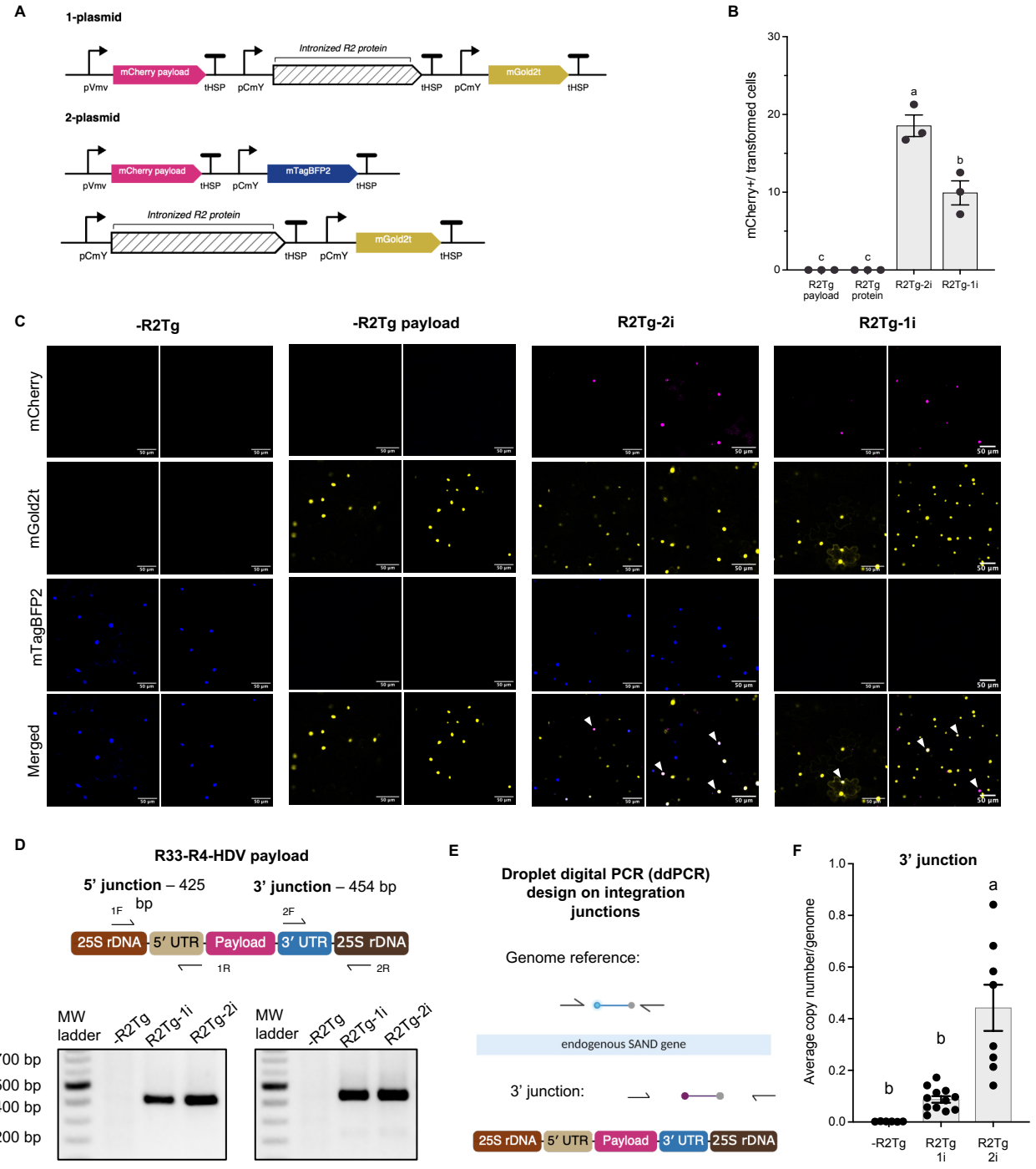

Supplementary Figure 13. R2Tg editor achieves targeted insertion in *Solanum lycopersicum*. **(A)** Schematic of R4-HDV payload delivered via 1- vs 2-plasmid with mGold2t and mTagBFP2 transformation markers. Fluorescent proteins are nuclear-localized. **(B)** Quantification of mCherry+ nuclei from confocal images. Bars represent mean ± S.E.M. n=3 independent biological replicates. P values were obtained using ordinary one-way ANOVA with Tukey HSD multiple comparison test. Different letters denote statistically significant differences; exact p-values for all pairwise comparisons are provided in the Source Data file. **(C)** Representative confocal fluorescence microscopy images of tomato leaves transformed with constructs in panel A, imaged 3 days post-transformation. Scale bars, 50 µm. Arrows indicate nuclear-localized mCherry signal colocalized with the transformation marker. Representative of 3 independent experiments with similar results. **(D)** Schematic and results of 5' and 3' integrated junction PCRs detecting targeted insertion at the 25s rDNA target site. Representative of 3 independent experiments with similar results. **(E)** Schematic of ddPCR on the 3' integrated junction. **(F)** Quantification of insertion copy number per genome using ddPCR on the 3' junction, normalized with endogenous SAND reference locus. Bars represent mean ± S.E.M. n=6 (-R2Tg), n=12 (R2Tg-1i) and n=8 (R2Tg-2i) independent biological replicates. Statistical analysis is performed using ordinary one-way ANOVA with Tukey's HSD multiple-comparison test. Different letters denote statistically significant differences; exact p-values for all pairwise comparisons are provided in the Source Data file.

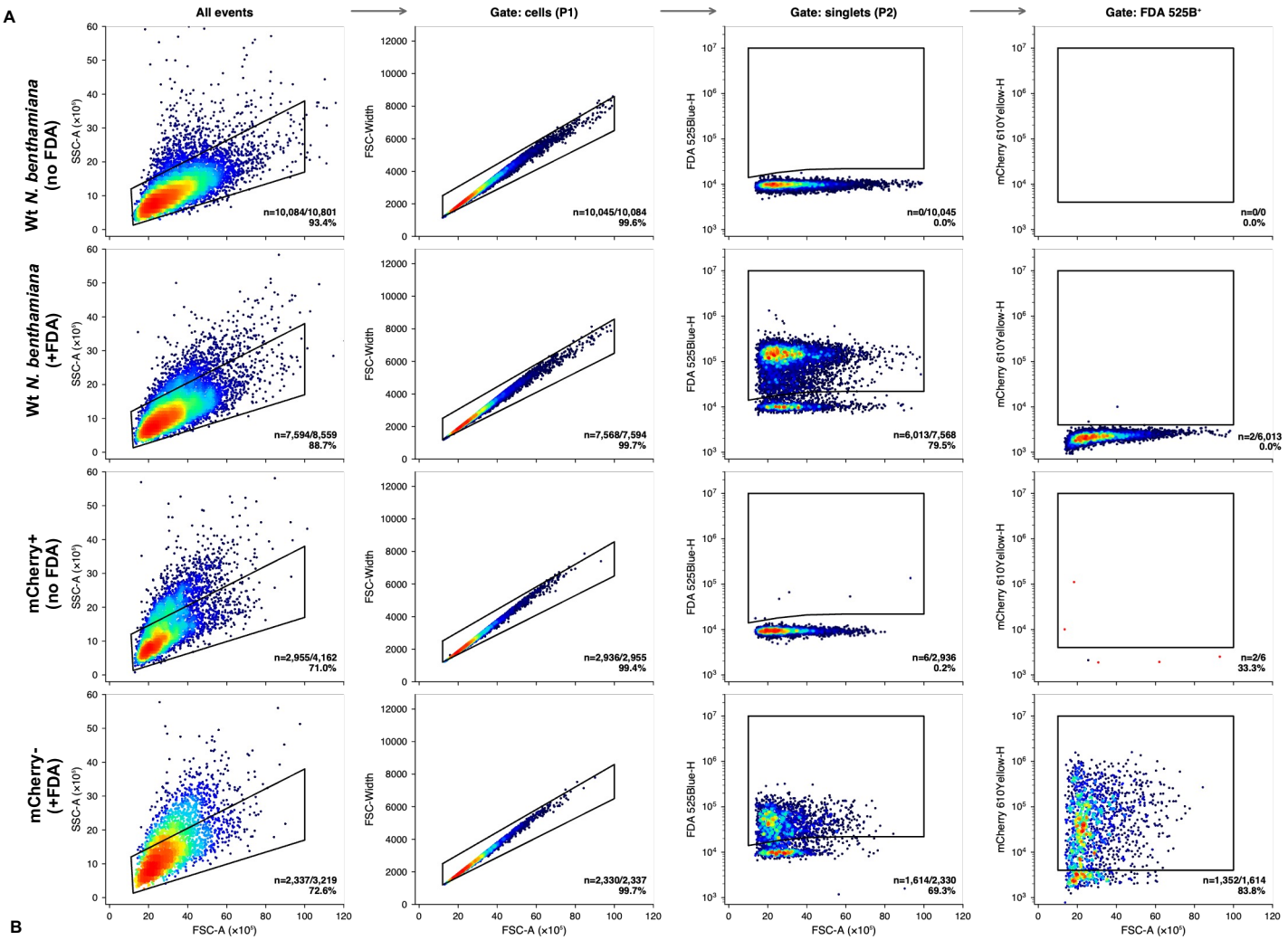

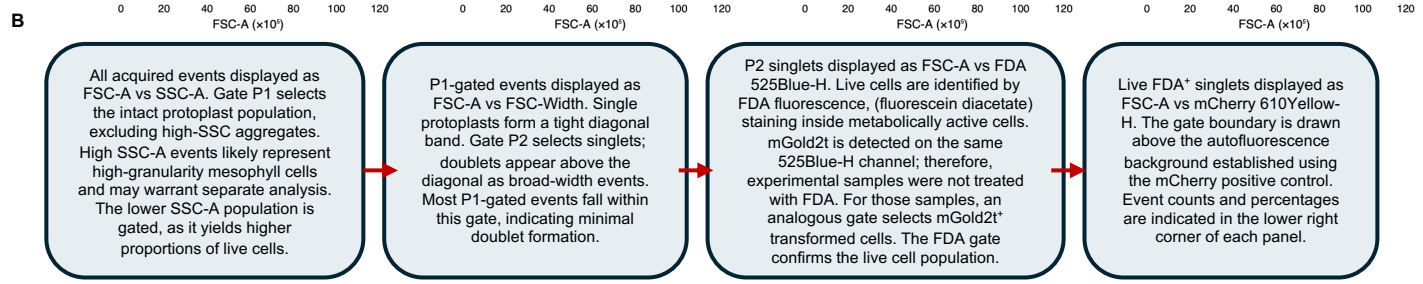

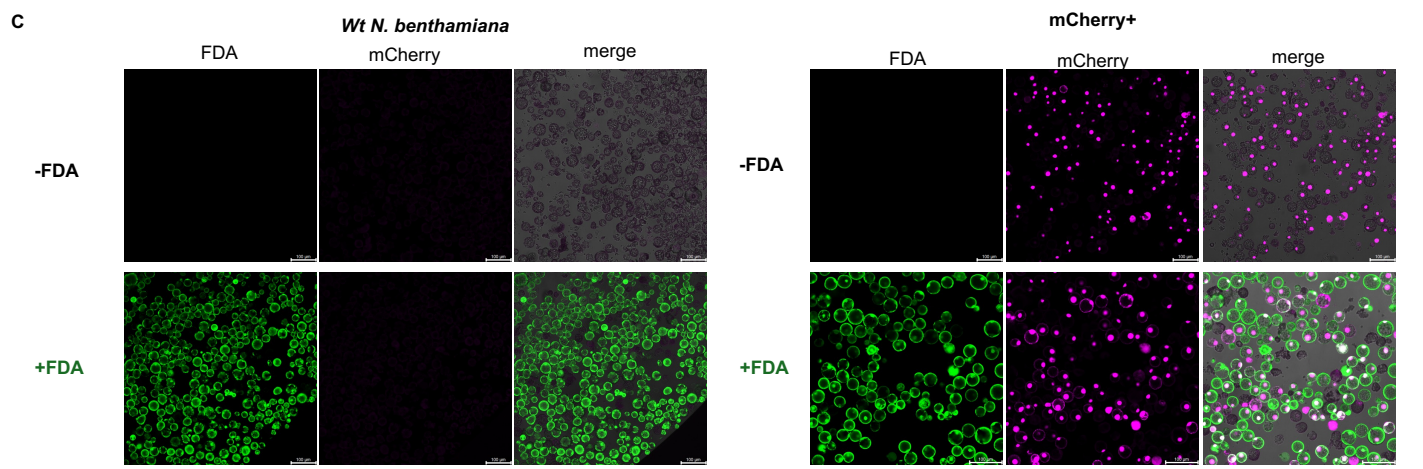

Supplementary Figure 14. Flow cytometry gating strategy for protoplast viability and mCherry detection.
(A) Sequential gating strategy applied to flow cytometry data from *Nicotiana benthamiana* protoplasts. Four samples are shown as rows: WT Nb (no FDA), WT Nb (+FDA), mCherry positive control (no FDA), and mCherry positive control (+FDA). Columns represent each step of the sequential gating hierarchy, with descriptions of each step provided in (B). Event counts and gate percentages are shown in the lower right corner of each panel. Representative of 3 independent experiments with similar results. **(B)** Descriptions of each gating step. **(C)** Representative confocal fluorescence images of *N. benthamiana* protoplasts from the mCherry positive control and WT Nb samples, with and without fluorescein diacetate (FDA) viability staining. mCherry fluorescence (magenta), FDA fluorescence (green), and merged channels are shown. Scale bars, 100 µm. Representative of 3 independent experiments with similar results. FSC-A: forward scatter area; SSC-A: side scatter area; FSC-Width: forward scatter pulse width; FDA: fluorescein diacetate; 525Blue-H: channel detecting FDA signal for cell viability and mGold2t fluorescence (excitation 488 nm, emission ~530 nm); 610Yellow-H: channel detecting mCherry fluorescence (excitation 561 nm, emission ~610 nm); mGold2t: monomeric gold fluorescent protein; mCherry: red fluorescent protein; WT Nb: wild-type *Nicotiana benthamiana*; P1: protoplast scatter gate; P2: singlet gate.

Figure 4. Increased integration efficiency and molecular validation via minimal homology length RNA templates with HDV ribozyme. (D) Target-junction PCR on genomic DNA isolated from infiltrated leaves. Expected band sizes for the 5′ and 3′ junctions are 425 bp and 454 bp. The R4-HDV minimal payload design paired with different R2Tg variants, including RT-dead and intronized versions.

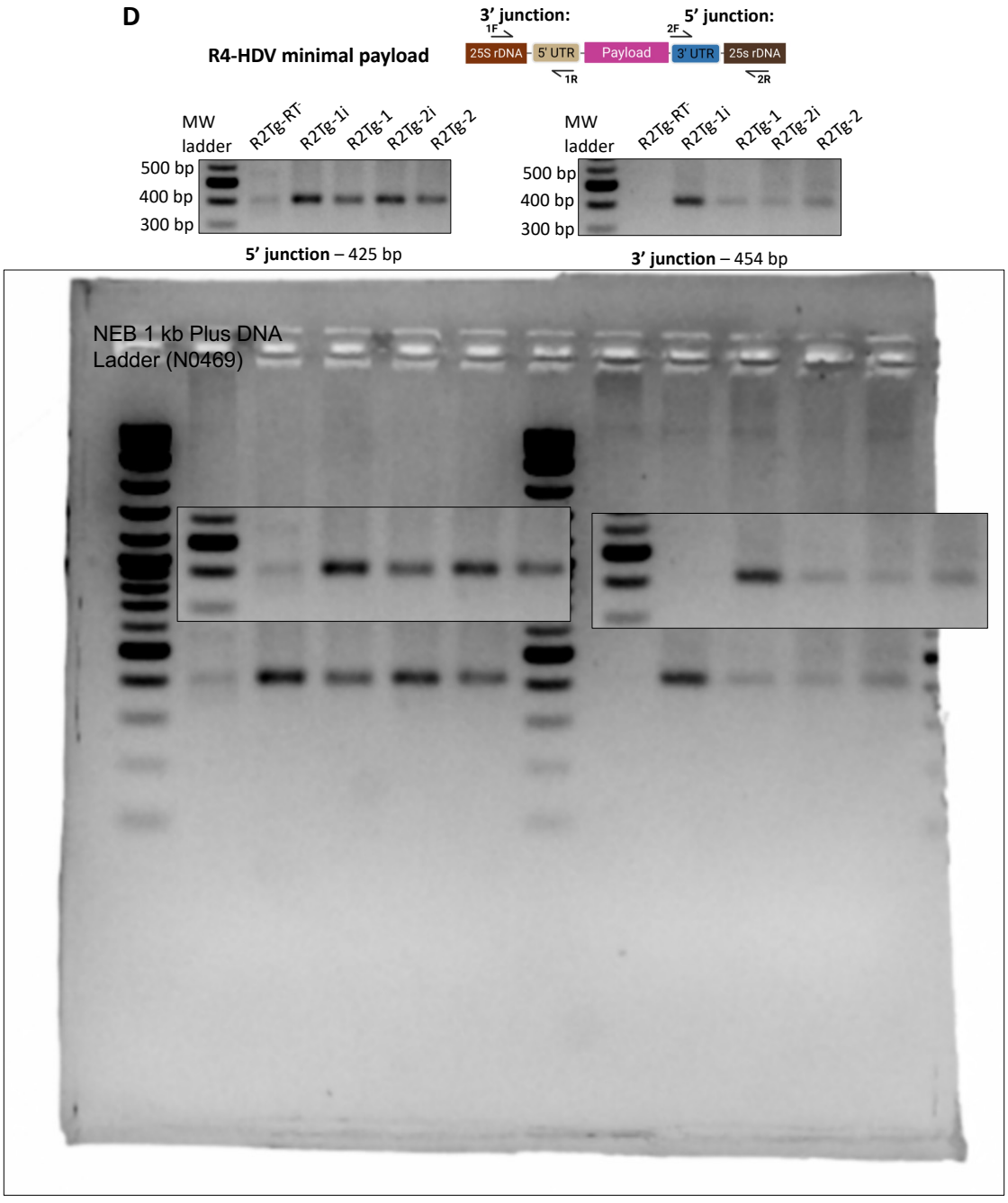

Figure 6. Optimized R2Tg editor system achieves efficient targeted insertion of a large DNA payload (D) Target-junction PCR on genomic DNA isolated from infiltrated leaves. Expected band sizes for the 5′ and 3′ junctions are 425 bp and 454 bp.

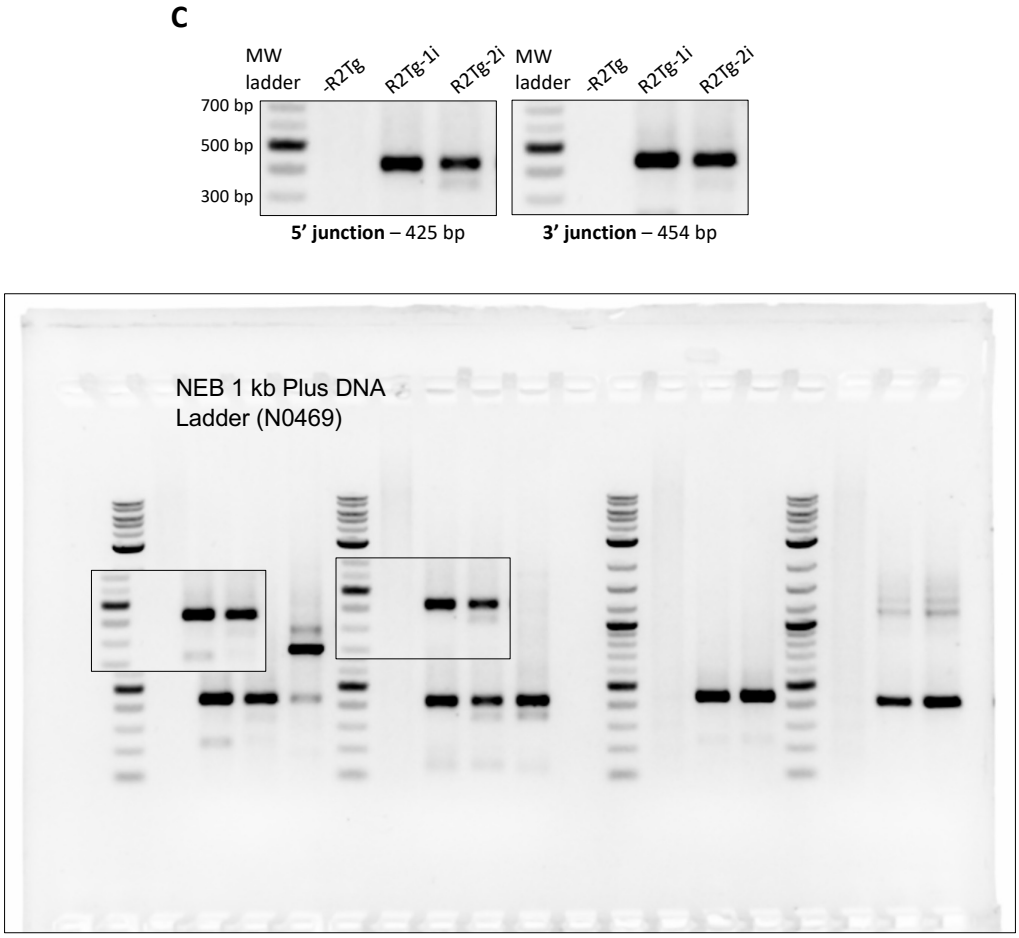

Supplementary Figure 1. Validation of 5′ UTR autocleavage activity and functional screening of R2 editors. (B) 2% TAE agarose gel showing cleavage products of three 5′ UTR variants: minimal *Tribolium castaneum* (minR2Tc), wild-type *T. castaneum* (wtR2Tc), and wild-type *Taeniopygia guttata* (wtR2Tg). Orange, blue and grey arrowheads indicate expected fragments. Band sizes match predicted cleavage outcomes: minR2Tc (uncleaved~177 nt, 105 nt, 72 nt), wtR2Tc (uncleaved~265 nt, 193 nt, 72 nt), and wtR2Tg (uncleaved~275 nt, 203 nt, 72 nt). A 300 nt synthetic RNA template was used to denote uncleaved template sizes

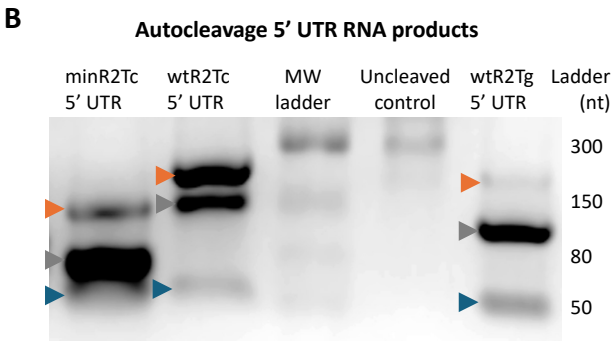

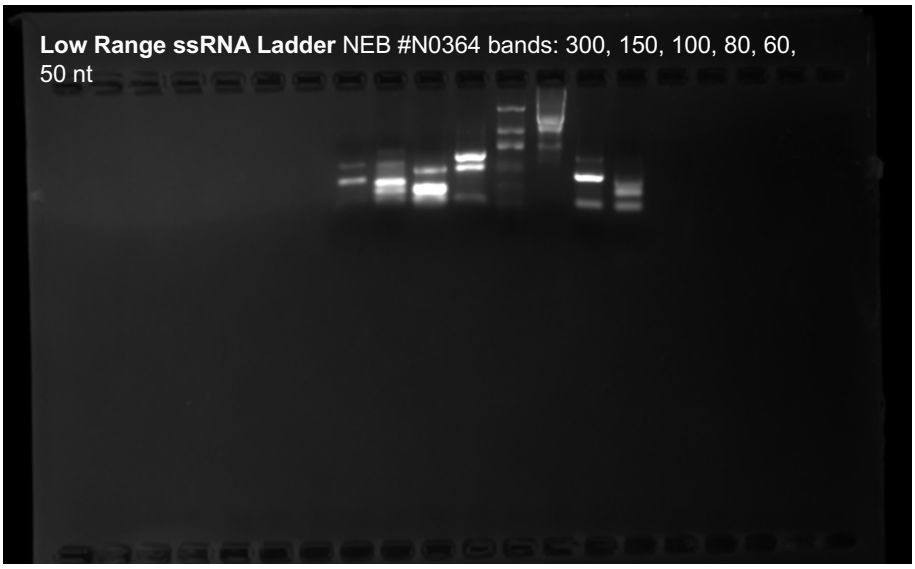

Supplementary Figure 9 | Characterization of R2-mediated payload insertion at the 25S rDNA locus in *Arabidopsis thaliana*. **(A)** Schematic of the 3' junction PCR amplicon (423 bp) used to detect R2Tg-1i-mediated targeted insertion, alongside a representative gel image showing amplification in R2Tg-1i-transformed plants but not the R2Tg control. The 3' integration junction site sequence is shown, with red arrows indicating the range of observed nick sites (positions −2 to +2) relative to the canonical cleavage site.

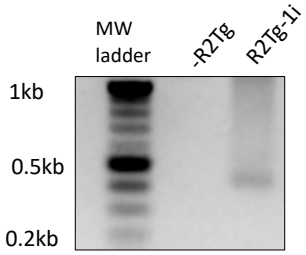

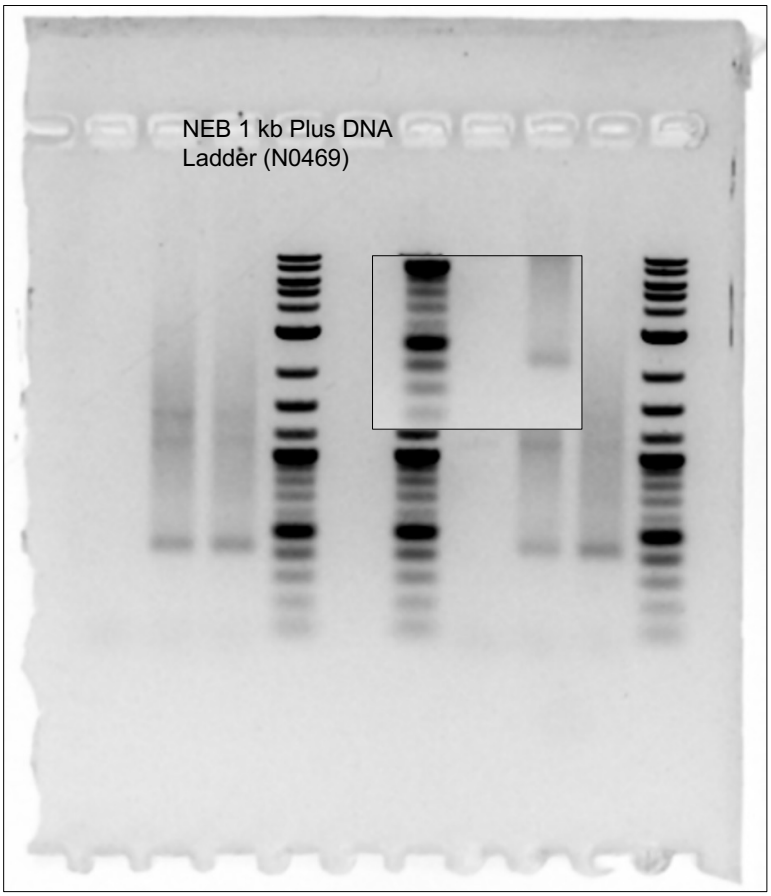

Supplementary Figure 10 |Cytosine methylation profile of integrated payload at the 25S rDNA target site in *Arabidopsis thaliana*. (B) Gel images confirming bisulfite conversion efficiency using primer pairs homologous to unconverted (BScontrol1) and bisulfite-converted (BScontrol2) DNA.

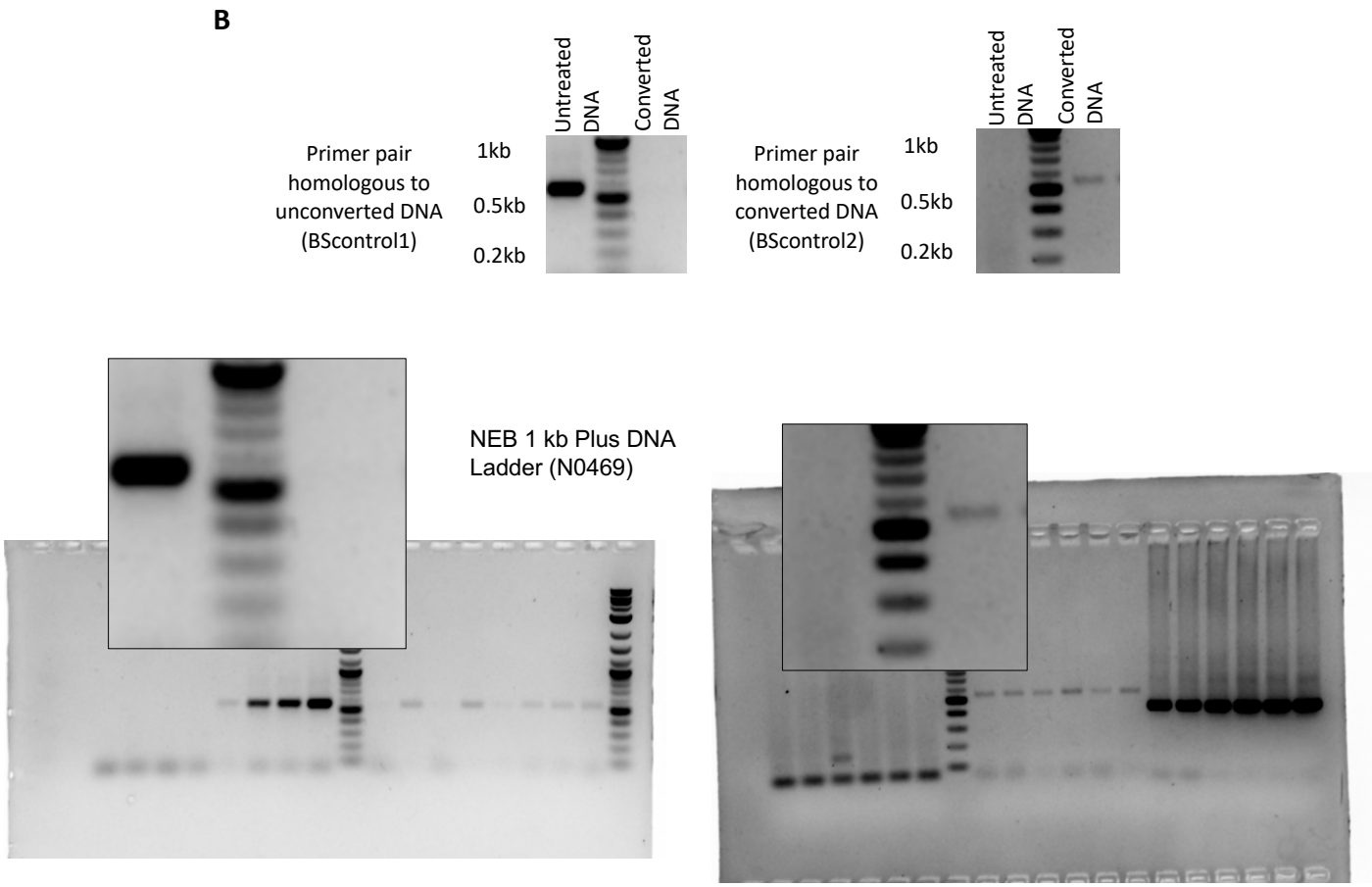

Supplementary Figure 13. Optimized R2Tg editor system achieves efficient targeted insertion in *Solanum lycopersicum.* (D) Schematic and results of 5’ and 3’ integrated junction PCRs detecting targeted insertion at the 25s rDNA target site in *S. lycopersicum*. **(E)** Schematic of ddPCR on the 3’ integrated junction.